44th AIAA Aerospace Sciences Meeting and Exhibit
9 - 12 January 2006, Reno, Nevada

X-43–Scramjet Power Breaks the Hypersonic Barrier Dryden Lectureship in Research for 2006

Charles R. McClinton
NASA LaRC (Retired), Hampton, VA 23681

NASA recently completed two major programs in Hypersonic Air-breathing Technology Development: Hyper-X, with the record-breaking flights of the scramjet-powered X-43; and the Next Generation Launch Technology (NGLT) Program. The major focus of this paper is the X-43 flight test results, implications of the X-43 results on technology status, and a recommendation on what NASA should do next. For background this paper summarizes potential benefits of air-breathing propulsion on NASA's space launch capabilities, as identified by NGLT. Highlights of the X-43 vehicle design and risk reduction process are discussed to set the foundation for ground to flight data and performance comparisons. Highlights of the flight test are presented including flight trajectory, experimental measurements and flight computer visualization. These measurements and results are compared with pretest (and some post test) analysis providing a major, essential demonstration of the capability of the airframe-integrated scramjet engine and hypersonic air-breathing vehicle design tools and vision vehicles. This paper also examines the significance of the flight test in advancing the state-of-the science (vis-à-vis technology readiness level) and provides a strategic vision for achieving, in the near future, the dream of safe, efficient, reliable and affordable space access achievable with air-breathing propulsion.

Nomenclature

ABLV	Air-breathing Launch Vehicle
AOA, Alpha, α	Angle Of Attack
Beta	Side slip angle
C-C	Carbon-Carbon
CFD	Computational Fluid Dynamics
C_L	lift coefficient
C_{Lo}	zero angle of attack lift coefficient
F2	Flight 2 (M = 7)
F3	Flight 3 (M = 10)
FEA	Finite Element Analysis
Fn/Wa	Thrust (lbs) per unit air flow (lbs/sec)
fps	feet per second
g	acceleration due to gravity
Isp	Specific Impulse
LEO	Low earth orbit
LOX	Liquid OXygen
L/D	Lift/Drag
LE	Leading edge
M	Mach number
NM	Nautical Miles
PF	Propellant fraction
PID	Parameter IDentification
psf	pounds per square foot
psi	pounds per square inch
Q	Pitch rate, deg/sec
q, Qbar	Dynamic pressure, psf
PF	Payload Fraction
$R_{e,\theta}$	Momentum thickness Reynolds number
S	vehicle reference area
SSTO	Single Stage To Orbit
T(R)BCC	Turbine (Rocket) Combination Engine
TOGW	TakeOff Gross Weight
TSTO	Two Stage To Orbit
T/C	ThermoCouple
TE	Trailing edge
TRL	Technology Readiness Level
T/W or Fn/Wt	Thrust-to-weight
V	Velocity
δ	horizontal tail (wing) deflection
$dC_L/d\alpha$	lift curve slope
$dC_L/d\delta$	lift change with elevator deflection

This material is declared a work of the U.S. Government and is not subject to copyright protection in the United States.

I. Introduction and Background

H. Julian Allen made an important observation in the 1958 21st Wright Brothers Lecture[1]**:** "Progress in aeronautics has been brought about more by revolutionary than evolutionary changes in methods of propulsion." Steam engines replaced sails and introduced mass transportation on the sea, and led to railroads. The internal combustion engine replaced the horse for private transportation, and led to the airplane. The jet engine replaced the piston engine, and revolutionized the airliner, taking it routinely above weather, and beyond seas. Modern rockets opened the space age for the bold and wealthy. In the 21st century, revolutionary applications of air-breathing propulsion will make space travel routine and intercontinental travel as easy as intercity travel is today. Development of technology for revolutionary propulsion systems for space transportation has long been a focus of NASA.

Figure 1 represents the first application of this revolutionary air-breathing propulsion technology to space access missions: an airliner-sized space vehicle[2] that serves as a high-speed, high altitude first stage launch platform for an expendable or reusable rocket-powered second stage. This modest approach significantly improves launch safety and reliability vis-à-vis existing systems. In addition, it initiates a new path for space access, with benefits which cannot be achieved with evolutionary improvements of current systems.

Benefits[2] of air-breathing launch systems are improved safety, mission flexibility, robustness and reduced operating costs. Safety benefits result from characteristics such as enhanced abort capability and moderate power density. Horizontal takeoff and powered landing allows the ability to abort over most of the flight, both ascent and decent. High lift/drag (L/D) allows longer-range glide for large landing footprint. Power density, or the quantity of propellant pumped for a given thrust level, is 1/10 that of a vertical take off rocket due to lower thrust loading (T/W), lower vehicle weight and higher I_{sp} (thrust/pound/second of propellant used—efficiency). Power density is a large factor in catastrophic failures. Recent analysis indicates that safety increases by several orders of magnitude are possible using air-breathing systems. Mission flexibility results from horizontal takeoff and landing, the large landing (unpowered) footprint and high L/D. Utilization of aerodynamic forces rather than thrust allows efficient orbital plane changes during ascent, and expanded launch window. Robustness and reliability can be built into air-breathing systems because of large margins and reduced weight growth sensitivity, and the low thrust required for smaller, horizontal takeoff systems. Current cost models indicate about one-order of magnitude reduction in operating cost is possible. These benefits are summarized in figure 2.

Development of safe, affordable, reliable, and reusable launch vehicles holds great promise as the key to unlocking the vast potential of space for business exploitation. Only when access to space is assured with a system that provides routine operation with orders-of-magnitude increased safety and at affordable cost will businesses be willing to take the risks and make the investments necessary to realize this great potential. Rocket-powered vehicles are approaching their limits in terms of these parameters[2]; switching to a new approach is the only way to achieve significant improvements. Air-breathing vehicles, capable of hypersonic speeds, can transform access to space, just like turbojets transformed the airline business.

Figure 1. Revolutionary Launch.

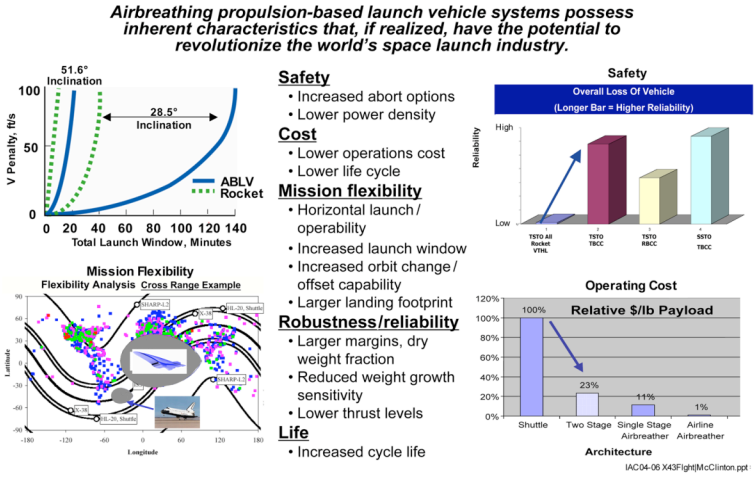

Figure 2. Benefits of Hypersonic Air-breathing Vehicles.

NASA has, for over 40 years (see figure 3), funded hypersonic airbreathing vehicle technology, aiming at futuristic space launch capabilities. This represents the next frontier in air vehicle design. In contrast, recent U.S. industry focus has been on avionics, stealth and methods to make the last generation of aircraft more effective. Evolutionary vehicle changes will give way to revolutionary changes when a new propulsion system is available. Studies by the Next Generation Launch Technology Program reconfirmed that hypersonic systems using turbine based "low speed" engines, combined with scramjets for higher Mach operation, up to at least Mach 7, and eventually to Mach 13-15, are the preferred long-term approach for air-breathing space access vehicles. Clearly, these turbine-based systems are also needed for supersonic cruise/hypersonic dash, or pure hypersonic cruise aircraft of the future.

NASA funded scramjet technology development, focused mostly on the propulsion cycle efficiency with numerous ground tests in wind tunnels (fig. 3) over the past 40 years[3]. Starting in the mid 60's, NASA built and tested a hydrogen fueled and cooled scramjet engine which verified scramjet cycle efficiency, structural integrity, first generation design tools and engine system integration. Starting in the early 70's, NASA designed and demonstrated, in wind tunnels, a fixed-geometry, airframe-integrated scramjet "flowpath" capable of propelling a hypersonic vehicle from Mach 4 to 7. Starting in the Mid 80's, NASA teamed with the DOD in the National AeroSpace Plane (NASP) Program to demonstrate hypersonic technologies required for a hypersonic, scramjet-based combined cycle powered, single-stage to orbit launch vehicle. Under the NASP program NASA focused on engine definition and testing for both the aerodynamic lines/cycle efficiency and hydrogen cooled engine structure.

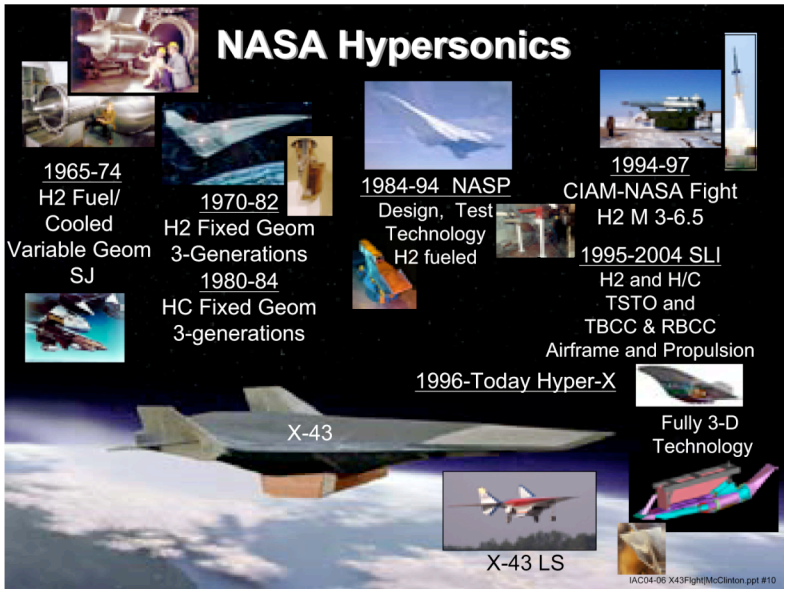

Figure 3. NASA History Perspective.

NASA developed the concept for the Hyper-X (X-43) Program in 1995-1996 as a result of several blue-ribbon panel recommendations that flight demonstrations of airframe-integrated scramjet-propulsion systems be the next major step in hypersonic research. The experts agreed that, at a minimum and as a first step, a vehicle must fly with an airframe-integrated supersonic-combustion-ramjet (scramjet) propulsion system. Consequently NASA initiated the Hyper-X program[1], a two phase program, with the first phase to demonstrate that scramjet engines can be designed, constructed, and operated at the high Isp levels necessary for use in access to space as well as to validate the design tools and methods to be used in the development of future hypersonic vehicles. The program phase 1 goals were established to provide performance data to reduce development risks for subsequent, operational vehicles; to advance performance-prediction capabilities for air-breathing hypersonic vehicles; to flight-validate airframe-integrated scramjet performance and design methods, and to flight-demonstrate other selected, key technologies. The second phase was to develop, integrate and flight test the "low speed" turbojet engine with the scramjet forming a complete hypersonic combination propulsion system.

The NASA Hyper-X program employed a low cost approach to design, build, and flight test three small, airframe-integrated scramjet-powered research vehicles at Mach 7 and 10. The Hyper-X team developed the X-43 phase 1 vehicle[4] as a small-scale, hydrogen-fueled research vehicle to provide flight data for a hydrogen-fueled, airframe-

integrated scramjet engine**.** In addition, aerodynamic, thermal, structural, guidance, flush-air-data-system, and other data were to be obtained. This research vehicle flight data will validate or guide improvements in hypersonic vehicle design tools. Test plans called for boosting each of three X-43 research vehicles to the required test condition by a drop-away booster. The research vehicles were dropped from the NASA Dryden B-52, rocket-boosted to test point by a modified Pegasus first stage, separated from the booster, and then operated in autonomous flight. Tests were conducted at approximately 100,000 ft. at a nominal dynamic pressure of 1000 psf. The resulting 12' long vehicle is illustrated in figure 4. Development of the X-43 and its systems are well documented [5-16].

The main body of this paper concentrates on performance of the scramjet powered X-43 vehicle and flight data relative to pretest predictions and some limited posttest analysis. These comparisons are made to provide insight into the state of this hypersonic technology. Then the paper will address the technology readiness level and some thoughts on a recommended approach to move forward.

II. Flight Test Overview

The first Mach 7 flight was attempted June 2, 2001. This flight failed when the Pegasus booster went out of control early in the flight. The second and third flights were successfully conducted March 27 and November 16, 2004. This section provides an unclassified overview of results from the second and third flight of the X-43. Details of the launch vehicle development, verification and validation and integration, as well as flight operations are well documented[17-20].

The target trajectory for the second (Mach 7) flight is illustrated in figure 5. The launch vehicle was dropped from the B-52 flying at Mach 0.8 and 40,000 feet. The booster ignited after a 5-second free fall to about 39,500 feet. The launch vehicle executed a 1.9g pull-up, followed by a 0.7g pushover to achieve nearly level flight at 95,000 ft. altitude. Following burnout, stage separation, and X-43 vehicle stabilization, the engine opened for about 30 seconds: 5 seconds of fuel-off tare, 10 seconds of powered flight (at about Mach 6.83 and dynamic pressure of 980 psf), another 5-seconds of un-powered steady tare, followed by 10 seconds of Parameter IDentification (PID) maneuvers[21]. The PID maneuver was designed to provide flight data to quantify the aerodynamic stability and control parameters for the vehicle, including drag parameter to allow more accurate estimation of the engine thrust. After the open-cowl PID maneuver, the engine cowl closed, and the vehicle flew a controlled descent over 300NM to "splash-down" in the Pacific Ocean. PID maneuvers were flown at various Mach numbers as the vehicle descended and slowed down.

The third flight trajectory was somewhat different. The B-52 flight conditions were the same. However, the launch vehicle executed a 2.5g pull-up to a flight path angle of over 30 degrees, followed by 0.5g push over to achieve nearly level flight at 110,000 foot altitude. Following burnout, stage separation, and stabilization of the X-43 vehicle, the engine was opened for about 20 seconds: 3 seconds of fuel-off tare, 11 seconds of powered flight (at about Mach 9.68 and dynamic pressure of 930 psf), and another 6-seconds of un-powered steady tare. (No cowl open parameter identification maneuvers were performed due to cowl survival concerns that necessitated closing the cowl immediately following the cowl open tare.) The engine cowl closed, and the vehicle flew a controlled descent over 800NM to a "splash-down" in the Pacific Ocean. During the descent PID maneuvers were successfully performed at successive Mach number as the vehicle slowed down.

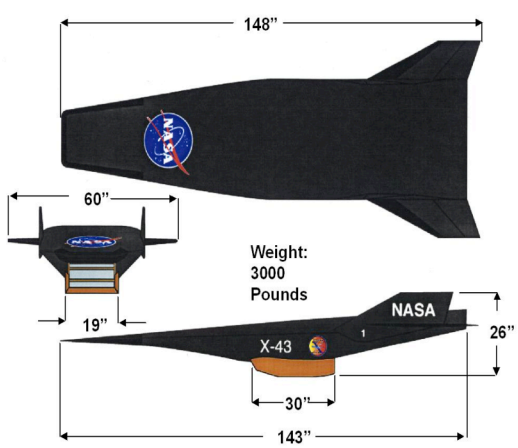

Figure 4. Three-View of X-43 Vehicle.

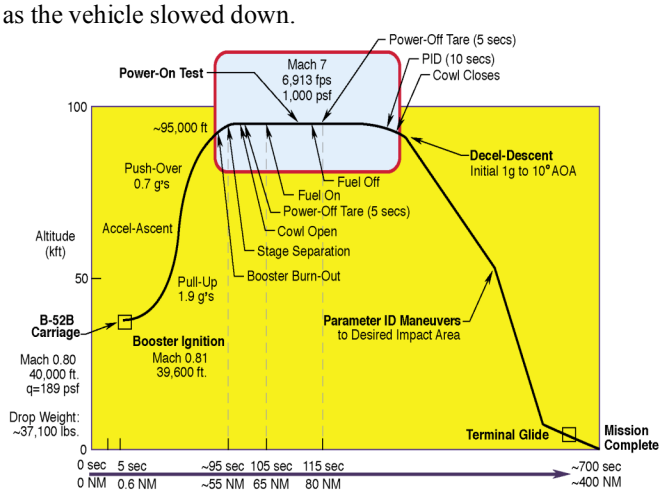

Figure 5. Pre-Flight 2 Design Trajectory.

The following discussion highlights flight 2 and flight 3 data and results from design-tool validation studies. The flight results contain much commonality, so the results are presented in terms of flight sequence and technology areas, including results from both successful flights. These are designated as F2 for the successful 2nd flight that targeted Mach 7 and F3 for the 3rd flight that targeted Mach 10.

III. Experimental Measurements

The X-43 vehicles were well instrumented. Instrumentation included over 200 measurements of surface pressure, over 100 thermocouples to measure surface, structural and environmental temperatures, and discrete local strain measurements on the hot wing and tail structures. The flight management unit included accurate 3-axis measurements of translational acceleration and angular velocity, along with Global Positioning System (GPS) and control surface deflection measurements. Instrumentation density is illustrated in figure 6 by external and internal wall pressure and temperature on the lower body surface. Internal engine instrumentation, within the cowl on the body side is denser to capture internal flow details within the engine.

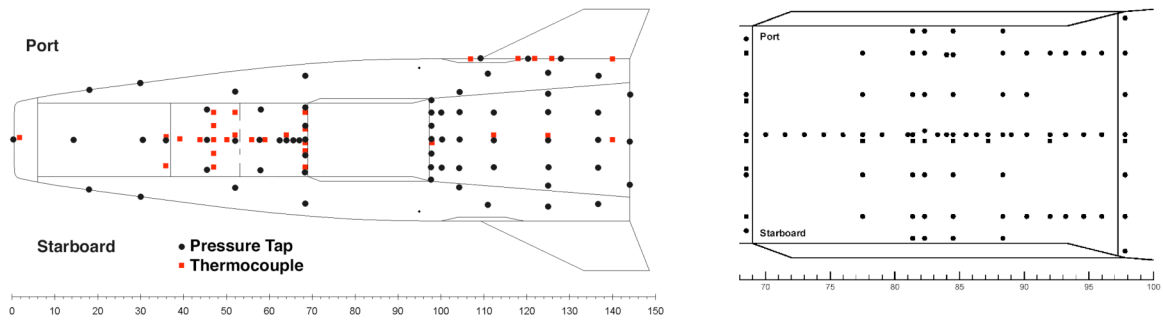

a) External **b) Internal**

Figure 6. Lower Surface Instrumentation.

All of the data from the X-43 flights were successfully telemetered and captured by multiple air and ground stations. The instrumentation health and performance were excellent: very few lost instruments/parameters; extremely low noise content; no significant calibration issues; no significant delay or time lag issues; and extremely limited telemetry stream drop outs. Accuracy of these measurements benefited from day-of-flight atmospheric measurements by weather balloons. These measurements were used in flight trajectory reconstruction[22], and resulted in a small change in calculated Mach number and dynamic pressure vis-à-vis real time values determined from atmospheric tables and winds from historical atmospheric tables. Flight 2 best estimated trajectories (BET) resulted in higher dynamic pressure and Mach, but only trivial change in AOA. Flight 3 BET resulted in lower dynamic pressure and higher Mach and AOA.

The flight test data from both flights F2 and F3 fully satisfied the Hyper-X Program objective to validate experimental, analytical and computational design methods. The X-43 flight data[23,24] was released to the U.S.`s hypersonic community in the spring of 2005.

A. Launch—Boost—Stage Separation

Development of the launch vehicle and execution of stage separation provided several well-documented challenges: most notably launch vehicle stiffness and vehicle control during separation. Launch vehicle modal frequency predictions were validated[25] using data gathered during the unpowered 5 seconds immediately following release from the B-52. First bending mode frequency values during this 5-seconds varied slightly, probably due to attachment preload strain energy, but the measured values (8.0 and 9.4 hertz for first modal pitch and yaw frequencies respectively) compare well, and slightly lower than predicted with the finite element analysis predictions (8.48 and 9.42 hertz).

Following the rocket motor burnout, the launch vehicle targeted 0° angle of attack (AOA-alpha) and yaw (Beta), zero pitch, yaw and roll rates, and 1000 PSF dynamic pressure for stage separation. The indicated Mach was slightly low. Post test analysis indicates that off-nominal rocket motor propellant temperature was the major factor affecting burnout and hence the reduced Mach number at F2 stage separation.

The research vehicle separation from the booster was executed cleanly (and was the first known successful high Mach, high dynamic pressure separation of two non-symmetric vehicles). The research vehicle angle-of-attack during the 0.3-second separation event, an indicator of understanding of the aerodynamic and piston forces, was within 0.2 sigma of the nominal prediction, validating models used in the 14 degree-of-freedom separation simulation. Cameras on board the booster captured a series of images of the research vehicle as it flew clear of the adapter. Figure 7 shows right and left cameras and a Booster/X-43 flight computer output-driven visualization of the right camera view. In this image, at 0.15 seconds from initiation of separation, the vehicles have separated by about 2 feet, and the all-moving horizontal control surfaces are moved to trailing edge down, to lift the vehicle as it passes the adapter. Also seen, are the separation pistons and linear variable displacement transducer (LVDT) wire used to measure vehicle separation distance and yaw. Additional details are included in the literature[26-28].

Figure 7. Stage Separation Camera and Visualization Images.

B. X-43 Free Flight

Following stage separation, the X-43 F2 research vehicle stabilized at 2.5° AOA, and the engine cowl was opened. After 5 seconds of tare force measurements, the engine was ignited with a pyrophoric silane-hydrogen fuel mixture (left photo in figure 8, then switched to pure hydrogen fuel for about 10 seconds of powered flight. The contrail from the pure-hydrogen fuel was not visible in the raw Halo tracking aircraft image (fig. 8).

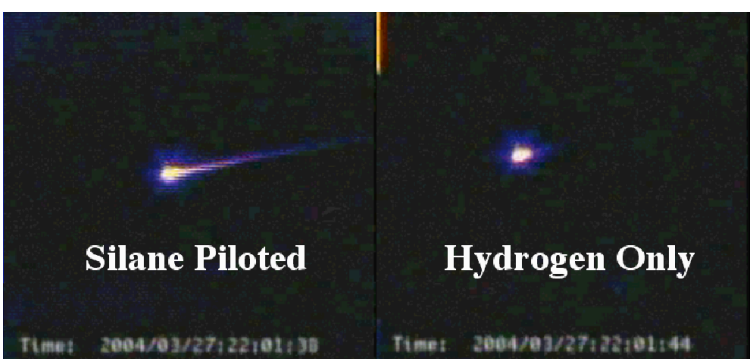

Figure 8. X-43 Powered Flight Video From Army Halo Aircraft.

Following the powered flight segment of flight 2, the vehicle performed a pre-programmed PID maneuver[21] with the engine cowl open, to quantify the aerodynamic stability and control derivatives, including drag parameters. Drag parameters were needed to correct the engine thrust estimate, because elevator deflection and angle of attack during the engine test were slightly different from the values during the tares, mainly because the thrust line was below the vehicle center of gravity (c.g.). Since both drag and thrust affect the longitudinal acceleration measurement used to determine engine thrust, drag corrections must be made to accurately determine engine thrust, and these corrections require the drag parameters. After the open-cowl PID maneuver, the engine cowl was closed, and the vehicle glided another 400 NM, and splashed down in the Pacific Ocean. PID maneuvers were flown at Mach 5, 4, 3, and 2 during the descent on flight 2. On flight 3, PID maneuvers were also performed during the descent, at Mach 8, 7, 6, 5, 4, 3, and 2. The descent segments of F2 and F3 provided a large, unique aerodynamic database for sharp leading edge lifting body configurations over a range of Mach numbers, and validated wind tunnel data and computational tools used to construct the X-43 aerodynamic database. F3 results presented in figure 9 illustrate the good agreement

between the pre-flight aerodynamic database and values determined from flight data[21]. The results shown are for two of the stability and control derivatives: a) lift curve slope $C_{L_\alpha} \equiv \partial C_L / \partial \alpha$, and b) drag due to elevator deflection $C_{D_{\delta_e}} \equiv \partial C_D / \partial \delta_e$. These parameters appear in the models for the non-dimensional force and moment coefficients:

$$C_L = C_{L_\alpha}\alpha + C_{L_{\delta_e}}\delta_e + C_{L_o} \qquad C_D = C_{D_\alpha}\alpha + C_{D_{\delta_e}}\delta_e + C_{D_o}$$

$$C_m = C_{m_\alpha}\alpha + C_{m_q}\frac{q\bar{c}}{2V} + C_{m_{\delta_e}}\delta_e + C_{m_o}$$

$$C_Y = C_{Y_\beta}\beta + C_{Y_r}\frac{rb}{2V} + C_{Y_{\delta_r}}\delta_r + C_{Y_o}$$

$$C_l = C_{l_\beta}\beta + C_{l_p}\frac{pb}{2V} + C_{l_r}\frac{rb}{2V} + C_{l_{\delta_a}}\delta_a + C_{l_{\delta_r}}\delta_r + C_{l_o}$$

$$C_n = C_{n_\beta}\beta + C_{n_p}\frac{pb}{2V} + C_{n_r}\frac{rb}{2V} + C_{n_{\delta_a}}\delta_a + C_{n_{\delta_r}}\delta_r + C_{n_o}$$

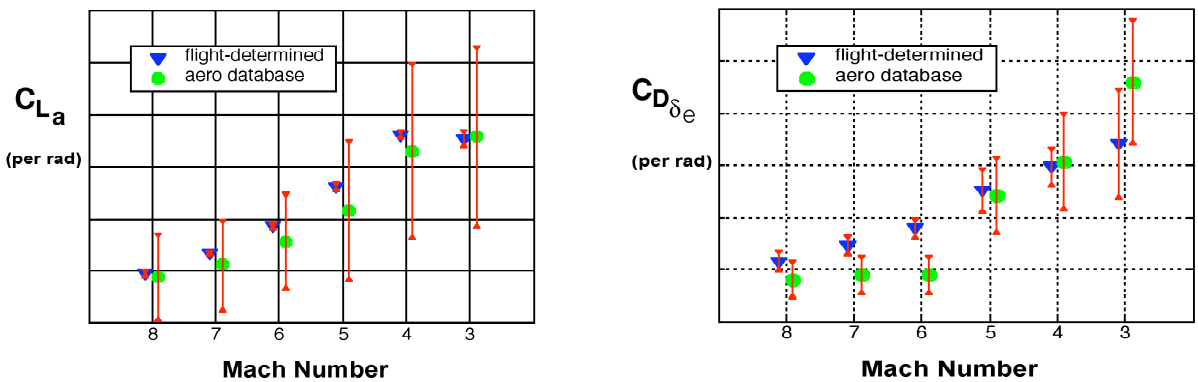

a) Lift Curve Slope, b) Drag due to Elevator Deflection,

Figure 9. Aerodynamic Parameters, Closed-Cowl Descent, Flight 3.

The bars in figure 9 represent 95 percent confidence intervals. The small uncertainty bounds for the flight results are indicative of the quality of the pre-programmed PID maneuvers, as well as good instrumentation, and low noise levels for the X-43 flying as a glider in smooth atmospheric conditions at high altitudes.

1. Scramjet Powered Vehicle Performance

For the Mach 7, flight 2, the X-43 was commanded to fly at 2.5° angle of attack during the cowl-open portion of the flight. However, as the fuel was turned-on/off, and throttle adjusted, the engine pitching moment changed significantly. Figure 10a illustrates the measured angle of attack—from cowl open to fuel off and the start of the Mach 7 PIDs. During the scramjet-powered segment, the AOA was maintained to 2.5° ± 0.2°, except during flameout, which occurred as the fuel was shut off. Some efforts were made in the flight control system to provide feed-forward control. For the Mach 10, flight 3, the vehicle was commanded to fly 1.0° angle of attack during the cowl open segment. The vehicle control was about the same (see figure 10b) during the powered segment as demonstrated in F2.

For both F2 and F3 the fuel sequencing for powered flight started with a silane/hydrogen mixture to assure ignition, then transition to pure hydrogen fuel. The ignition sequence for F2 required about 1.5 seconds. With transition to pure hydrogen fuel, the throttle is ramped up to either a predetermined or controlled maximum value (limited by inlet unstart monitor), and then decreased as the fuel was depleted. The resulting vehicle performance is characterized by vehicle acceleration, as shown in figure 10. The ignition sequence for F3 was different—the silane remained on for the first two fueled conditions, requiring 5 seconds of silane pilot. Then the same equivalence ratio test conditions were run with only hydrogen. This cautious approach was taken because it was not possible to transition from piloted to un-piloted operation in the short test time available for tests performed prior to the flight test in shock tunnels.

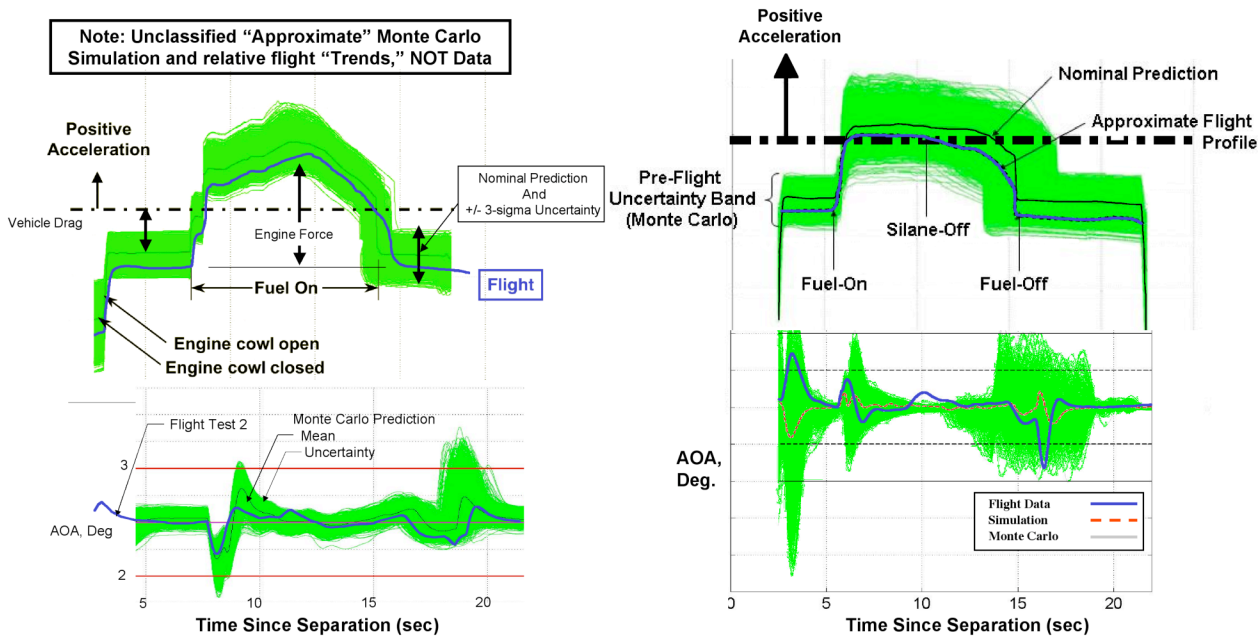

a) Mach 7, Flight 2 **b) Mach 10, Flight 3**

Figure 10. X-43 Axial Acceleration and Angle of Attack During Powered Flight.

Green bands in figure 10 illustrate pretest Monte Carlo predictions of acceleration and angle of attack (using unclassified representative propulsion database). The heavy blue line depicts flight data trends. The vehicle deceleration is greater than predicted[29,30], both with cowl closed and open. This is because of two factors: 1) actual flight conditions (2/3 of the difference), and 2) vehicle drag was higher than predicted (1/3 of the difference). However, the drag was within the uncertainty associated with the aerodynamic database[31]. The uncertainty was not resolved before flight because it did not threaten the outcome of the engine tests. These flight data will be used to help reduce the aerodynamic database uncertainty for future missions.

Under scramjet power the F2 vehicle acceleration was positive, and varied with throttle position. The increment in acceleration is about as predicted, which confirms the predicted engine thrust to within less than 2% (ref. 5 and 6). It should be noted that the engine throttle was varied over a large range without incurring engine "un-start" or "blow-out." Under scramjet power the F3 vehicle cruised (thrust = drag) at the reference fuel equivalence ratio with 2% silane pilot, and the engine force was in agreement with predictions[32].

Predicted scramjet performance is also confirmed by the excellent comparison of pre-test predicted and flight scramjet flowpath wall pressure (fig. 11). Data are presented from vehicle nose to tail for F2 (fig. 11(a)), and from cowl leading edge to cowl trailing edge for F3 (fig. 11(b)). Mach 7 data showed the scramjet operating in "dual mode," with sonic flow in the isolator dissipating the inlet shocks. Mach 10 data exhibits classical pure supersonic combustion mode, i.e. the combustor pressure is shock dominated. The pretest prediction for Mach 7 was made using the SRGULL code, with combustion efficiency determined by analysis of multiple wind tunnel tests, most notably, the 8' HTT test of the Hyper-X Flight Engine (HXFE) on the Full Vehicle Simulator (FVS). The Mach 10 pretest prediction was performed using a combination of CFD tools, with the SHIP code used for the combustor. (SRGULL was also used to predict engine performance at Mach 10, but SHIP was the primary code due to the shock-dominated flow which is not captured with SRGULL). The reaction efficiency used in the SHIP code was derived from analysis of engine tests conducted in the HYPULSE and LENS reflected shock tunnels. Storch[5] and Ferlemann[32] present a detailed discussion of these codes and the pretest predictions for F2 and F3 respectively.

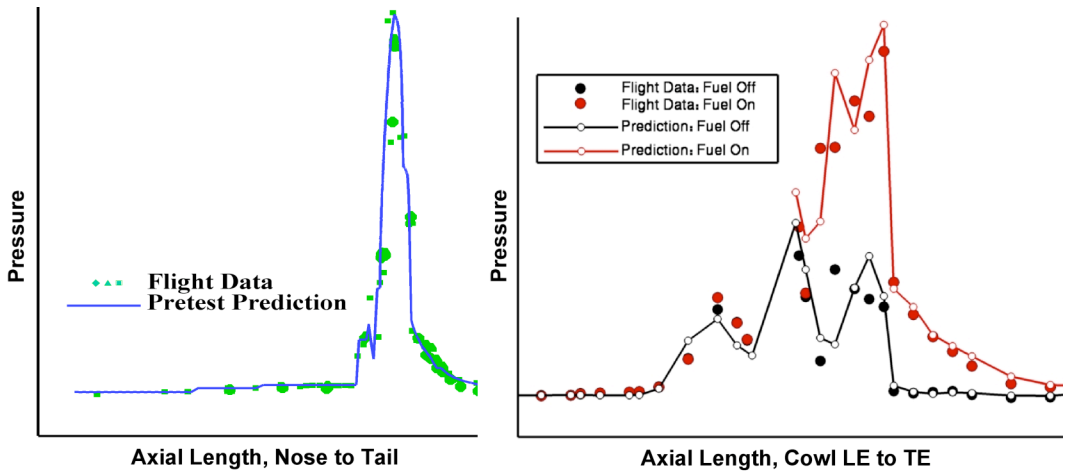

a) F2, Mach 6.83. **b) F3, Mach 9.68.**

Figure 11. X-43 Flowpath Pressure Distribution: Design Throttle Position.

C. Wind Tunnel / Flight Scramjet Comparison

F2 flight data compare favorably with measurements made in four separate wind tunnel tests[7,33] and F3 flight data compare favorably with results from both the HyPulse and LENS shock tunnel tests[33]. Tests with nearly identical fuel equivalence ratios were selected for comparison. Wind tunnel wall pressures were scaled by air mass capture ratio to flight conditions. Figure 12 illustrates the resulting comparison of internal wall pressure for the 8' High Temperature Tunnel (HTT) test of the Hyper-X Flight Engine (HXFE) on the Full Flight Vehicle Simulator (FFS). Similar agreement was noted between flight data and data produced using semi-direct connect engine module tests in shock heated, combustion heated and electric arc heated wind tunnels. Storch[5] discusses the implication of this agreement, and the impact on observed combustor performance. Rogers[34] reported a similar trend for the Mach 10, flight 3 data. Results show that ground tests are representative of flight when careful attention is paid to modeling the appropriate flow phenomena. The most significant issues identified for shock tunnel testing are wall temperature limitation and attention to correct shock position entering the combustor for shock-dominated "pure" scramjet operation.

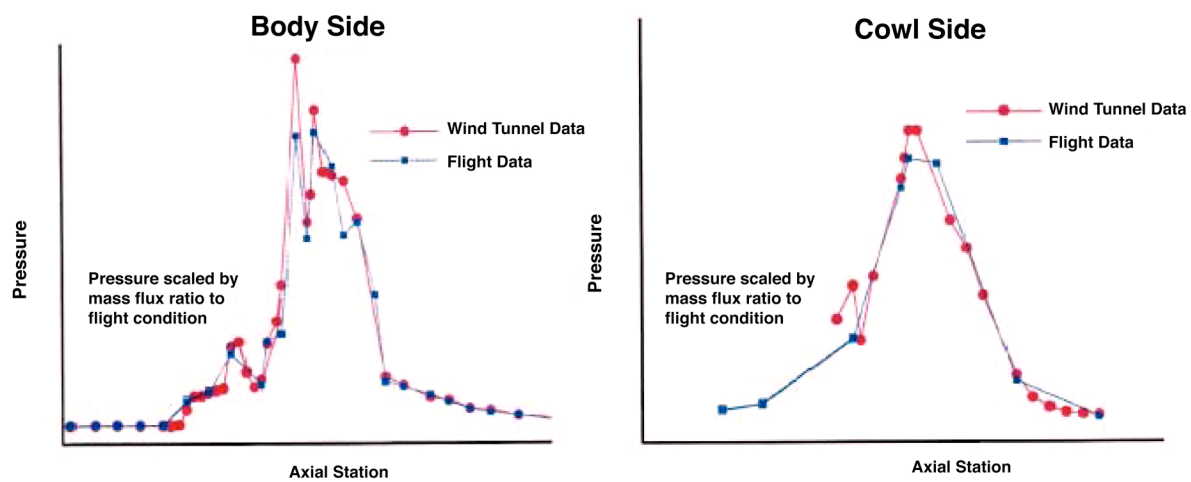

Figure 12. X-43 F2 Flowpath Pressure Distribution: Design Throttle Position.

D. Aerothermal, Thermal-Structure Analysis and Boundary Layer Transition

The design of the X-43 research vehicle structure and thermal protection system depended greatly on accurate estimation of the aerothermal environment, which required understanding of the boundary layer state during the entire flight. For good engine operation, boundary layer flow entering the inlet cannot be laminar. For the X-43, boundary layer trips were required to insure the forebody boundary layer was turbulent for mitigation of any flow separations along the

engine flowpath due to adverse pressure gradients. A substantial research and design effort[31] was executed to ensure proper sizing of the trips with minimum induced trip drag. The upper surface, however, was predicted to be laminar during the Mach 7 test point, based on a pre-flight trajectory, using a classical correlation methodology (momentum thickness Reynolds number over the boundary layer edge Mach number of $R_{e,\theta} / M_e = 305$).

Figure 13 provides upper surface temperature time histories during the first 350 seconds of flight 2 trajectory from the point of release from the B-52. The three upper surface thermo-couples were evenly spaced along the vehicle centerline starting about midpoint for T/C#19 and ending near the trailing edge for T/C#21. Note that by the time the cowl opens and the scramjet is ignited, the entire upper surface appears to be laminar, as indicated by the dramatic temperature decrease that begins at about 70 sec. Likewise, at about 240 seconds the boundary layer transitions from Laminar to turbulent as the vehicle slows. The pre-flight predictions, using the classical approach, were accurate (300±12) in estimating these latter transition points along the flight trajectory. However, the transition from turbulent to laminar earlier in the flight occurred at a local $R_{e,\theta} / M_e = 400$. Thus the laminar-to-turbulent and turbulent-to-laminar transition criteria are not the same, and the X-43 measurements provide flight data that quantify the hysteresis effect[35].

E. Thermal Loads

Preliminary and continuing assessments of thermal loads for the F2 and F3 flights, compared with design values, are documented in various sources[36-39]. These documents show that the conservative engineering approach used in the design and development of the flight vehicles was generally just that—conservative. However, some temperature measurements, in regions of steep gradients, were higher than anticipated, particularly late in the boost. The effect of "actual boost trajectory" vs. "design trajectory" is continuing to be studied. Results to date generally confirm prediction methods. Accuracy of the predictions appears significantly better than the assumed uncertainty for both Mach 7 and 10 flights. For example, figure 14 illustrates heating to the leading edge of the vehicle predicted using the "as flown" trajectory, with measured temperature within the C-C leading edge material. Adjacent nodes from the FEA model bracket the measured temperatures over the boost and scramjet powered flight at Mach 10.

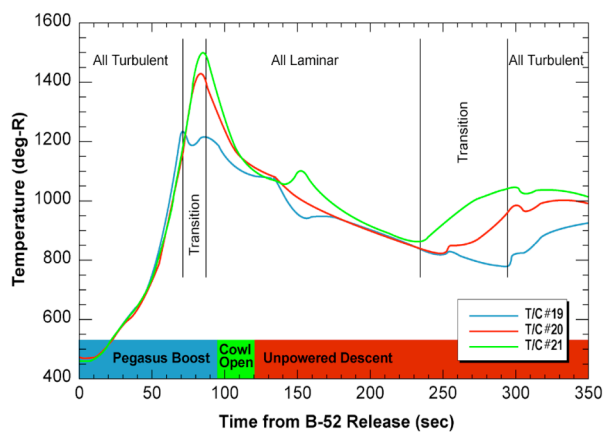

Figure 13. X-43 Upper Surface Temperatures from B-52 Drop to Splash.

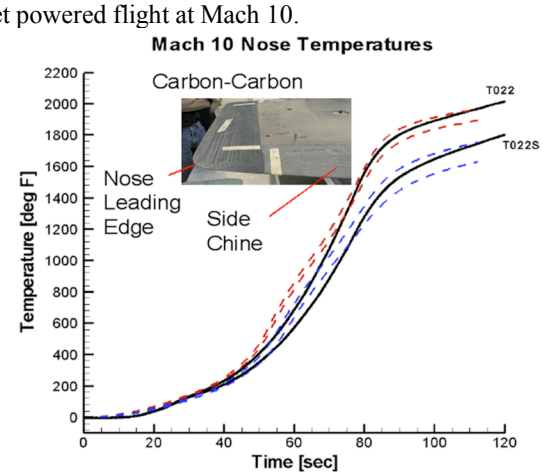

Figure 14. Nose LE temperature confirms Thermal model.

F. Post Test Analysis

Post test analyses of the flight data are underway at NASA Langley Research Center[40,41] and elsewhere. Some of these analyses are required to model the "as flown" trajectory to properly assess thermal loads, to assess inlet mass capture at exactly the flight condition achieved, to evaluate the true boundary layer state for boundary layer transition assessment, and to assess the overall vehicle drag, engine force, and vehicle acceleration/deceleration at exact flight conditions/control positions. Complete nose-to-tail CFD solutions for the actual flight condition include solutions for cowl closed (fig. 15a), cowl open (fig. 15a), and powered operation (fig. 15b). These solutions show excellent agreement (fig. 15c) with measured acceleration/deceleration.

Another post test analysis[42] determined the engine efficiency (specific impulse–I_{SP}) achieved, and then extrapolated or "scaled" that value to a vision vehicle, removing effects of small physical scale, cold fuel, off-nominal fuel equivalence ratio, operating dynamic pressure, etc. Unclassified results[42] are presented in figure 16. The specific

impulse is within the capability band projected for scramjet engines. The specific and effective impulse demonstrated in this scaling study will certainly set the standard for follow-on vehicle configurations.

X-43 flight data validated design tools for scramjet, aero and aerothermal performance. Included in this hypersonic environment are many physics challenges, such as natural and forced boundary layer transition, separation caused by shock-boundary layer interaction, shock-shock interaction heating (type 3 and 4), isolator shock trains, cold-wall heat transfer, fuel injection, penetration and mixing, finite rate chemical kinetics, turbulence-chemistry interaction, boundary layer relaminarization, recombination chemistry, and catalytic wall effects. Most of these phenomena were modeled in the design tools. Others were avoided by application of a large uncertainty. Success of the X-43 demonstrates an engineering level understanding of these physic issues. A better understanding of these issues might be beneficial in optimization of vehicle performance—but the current understanding is clearly adequate to continue higher-level technology development and integration. Tools developed and demonstrated in the Hyper-X program are applicable, and representative of the best available, for future design concepts.

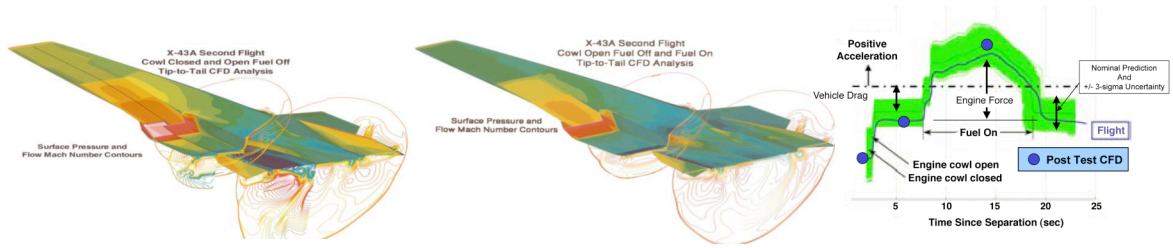

a). Unpowered; Cowl Closed and Open Tare **b) Fueled** **c) Comparison with Flight Acceleration**

Figure 15. X-43 Post Test CFD Solutions.

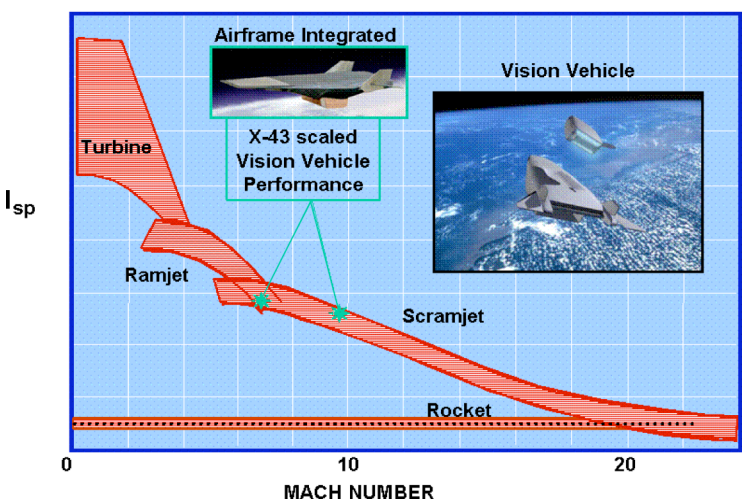

Figure 16. X-43 I_{SP} Scaled to Vision Vehicle.

IV. Phase 2 Technology Plan

The successful Mach 7 and 10 flight tests of the Hyper-X/X-43 research vehicle provided major, essential demonstrations of the capability of hypersonic air-breathing vehicle design tools and, by implication, vision vehicles. Technology advancements made by this flight test could not have been made using just wind tunnels and CFD. This flight was a small but crucial step toward maturing air-breathing hypersonic propulsion for application to space-launch vehicles and other efficient hypersonic systems. This is only the first of many flight tests which must be performed, in conjunction with wind tunnel tests, systems analyses and engineering, and basic research, before the technology will be fully ready (Technology Readiness Level or TRL = 6) for practical applications to future vehicle systems. This section examines the significance of the flight test in advancing the state-of-the science (TRL) and provides a strategic vision for achieving the goal of safe, efficient and reliable space access with air-breathing propulsion, through focus on technology for near-term vision vehicles.

A. Technology Readiness Level (TRL)

Significant advancements in hypersonic technology have been made over the past 40 years. These technologies address hypersonic airframe, engine and systems development. The state of technology, expressed by a rating called *Technology Readiness Level* (TRL), was documented by the National Aerospace Plane Program[43] (NASP), NASA's Hyper-X program[44], NASA's Next Generation Launch Vehicle Technology (NGLT) program[45], the 2004 National Research Council (NRC) review[46] of The National Aerospace Initiative (NAI) Hypersonic Pillar, and a Boeing Senior Fellows Review of Hypersonic Technology[47]. A typical vehicle-based work breakdown structure (WBS) used to guide TRL tracking of hypersonic launch vehicle technology development progress developed by NASA's NGLT Program is presented in Appendix A of reference 48, and will be drawn on for this discussion.

All of the technology development summaries[43-47] address the technology needs of an "ultimate" air breathing launch system: it utilizes air breathing propulsion from take off to at least Mach 12-15—in either a single- or two-stage to orbit architecture. These vehicles are exposed to extreme thermal loads, and require the most advanced technologies for engine, vehicle structures and thermal protection system (TPS). TRL status, including X-43 advancements, for typical vehicles operating in these environments is illustrated in figure 17. Bowcutt[47] substantiated this with his list of "critical and enabling technologies" for the high-Mach application of air-breathing as: "air-breathing propulsion; high temperature materials and thermal protection Systems (TPS); reusable cryogenic tank and integrated airframe structures; and integrated vehicle design and multidisciplinary design optimization (MDO) tools." These are generally shown as lower TRL (3-4) in figure 17, for high Mach (15) air-breathing systems.

Figure 17. TRL Status for High Mach Air-breathing Systems (Mach 15 Air-breathing SSTO).

After such a successful flight test of a scramjet-powered vehicle, the question may arise, how can the TRL for scramjet propulsion (WBS 2.01) only be 3-4? Scramjet flowpaths required to operate from Mach 4 to Mach 15 are not fully demonstrated in a relevant environment by a single flight test at Mach 7, or even Mach 7 and 10. The engine concept must be tested at reasonable Mach increments from Mach 4 to 15. TRL remains low especially at the very high speed end, where ground testing is limited to expansion tunnels with run times on the order of 1 ms. Estimates of the time and cost required to complete this "ultimate" technology set are documented by many sources, most notably the USAF Scientific Advisory Board (SAB)[49].

Fortunately, system studies show alternate approaches, with less ambitious technologies, can meet many of NASA's goals for safe and affordable launch. Typical payloads for a 1.2-1.5Mlb TOGW two-stage vehicle (*Antonov An-225*-size/weight) with reduced staging Mach number, expendable second stage and moderate technology are illustrated in figure 18. In fact, NGLT assessments concluded that 80% of the current and projected world payloads are 20,000 pounds or less (PF < 2%).

Attributes for selected air-breathing assisted launch systems categorized by staging Mach number and reusable or expendable second stage are listed in figure 19. NASA's NGLT Program identified and quantified these attributes[2,50]. For example, staging at Mach 7, and using an expendable second stage allows nearly an order of magnitude gain in safety (loss of vehicle/payload), with a small improvement in payload fraction and operating cost, compared with current systems (Space Shuttle or ELV's). Increasing staging Mach number (the fraction of air-breathing contribution to orbital velocity) plus adding a reusable second stage and more advanced engine and airframe technology, increases the payload fraction and reliability, and reduces both loss of vehicle (LOV) and operating cost. The most significant benefit is in safety, quantified by the attribute "Loss of Vehicle." Safety benefits are estimated at up to a 3 orders of magnitude increase compared to existing systems[2].

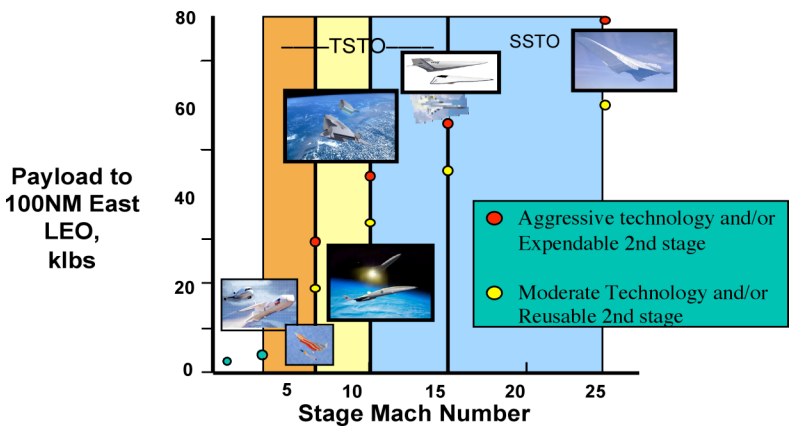

Figure 18. Air-breathing Launch Systems Capabilities.

Attributes	Baseline ELV	Baseline Space Shuttle	Mach 7 Stage[9]	Mach 10[1]	Mach 15	SSTO[1]
	Expendable	Partially reusable	Expendable 2nd stage	Reusable	Reusable	Reusable
Payload Fraction	3%	1%	2-3%	3%	4%	5%
Loss of Vehicle/Payload	1:50	1:100	1:4,000	1:60,000	1:110,000	1:160,000
Cost per Lb to LEO	$2,500	$10,000	$1,700	$2000	$1400	$1000

Figure 19. Benefits of Air-breathing Launch Systems.

Airframe and propulsion subsystems performance (goals) required[48] to develop the vehicles characterized in figures 18 and 19 are illustrated in figure 20. These vehicles utilize turbines for low-speed operation, and ramjet and/or scramjet for higher speed operation. The integrated engine is referred to herein as a "Turbine-Based Combination Cycle" (TBCC) engine. Lower staging/air-breathing limit concepts were assumed to have less challenging technologies—such as airframe dry mass fraction, turbojet operating Mach limit/efficiency (Isp), weight (T/W), and engine and airframe durability/life. Mach 7 vehicle concepts utilize dual-fuel: i.e. JP for turbojets and liquid Hydrogen for the ram/scram engine. TBCC engine cycle transition is set at realistic limits for existing turbojets, Mach 2-2.5. Existing turbojets (TRL=9) may be used for low-speed, and conventional ramjets (TRL=9) operate well from Mach 2 to over Mach 5, and have been demonstrated in regenerative-cooled ground tests[51] with liquid hydrogen to Mach 8. This Mach 7 concept uses variable geometry as demonstrated by the French Wide Range Ramjet (WRR) Program[52] to transition from conventionally throated ramjet to thermally throated dual-mode scramjet operation. Transition from turbine to ramjet mode at low Mach number (2.0-2.5) is less challenging than for the higher Mach number vehicles, which transition at Mach 3.5 to 4. These higher Mach number configurations also require an advanced turbojet, like the Revolutionary Turbine Accelerator (RTA) engine project started in the NASA NGLT program.

Technology status for the Mach 7 first stage vehicle is summarized in figure 21. Clearly the technology set for a Mach 7 vehicle is less challenging than for the SSTO or high Mach air-breathing first stage of a two-stage to orbit concepts (figure 17). For example, all of the airframe technologies are at least TRL 5-6 and required propulsion performance is at least TRL 5-6. In addition, some technology areas, such as LOX addition (WBS 2.03) are not required for this class of vehicle. "NA" notates these areas in figure 21. Programs to complete the technology in figure 21 to TRL 6 were recently estimated by a NASA planning activity to be an order of magnitude less cost and 1/3 of the time required for the most advanced technology set identified in figure 17.

	Airframe		Propulsion						
Airbreathing Limit, Mach	Dry mass fraction	Life, flights	Cycle	Fuel	Mach	ISP	Fn/Wa	Fn/Wt	Life, Flights
7	0.42	100	Turbine	H/C	0 1.2 2.5	2500 2000 1900	140 120 80	7.5	100
			TBCC Integration	Dual	2.0-2.5	TBD	80	3.2	
			Ram/Scram	H2	2.5 6	3400 2900	110 95	15	
10	0.38	500	Turbine	H/C	0 1.2 4	2500 1900 1600	140 125 100	10	500
			TBCC Integration	Dual	3.5–4.0	TBD	75	Installed TBD	
			Ram/Scram	H2	4 8	3000 2800	95 90	15	
15	0.33	2000	Turbine	H2	0 1.2 4	5500 5000 4400	140 125 100	15	2000
			TBCC Integration	H2	3.5–4.0	TBD	75	Installed TBD	
			Ram/Scram	H2	4 8 15	3200 2900 1400	95 90 55	12	
			RBCC	H2-O2	15 22	750 650	135 90	12	

Figure 20. Subsystem Goals.

B. Mach 7 First Stage Technology Shortfalls

Details of the technology shortfalls (TRL < 6) in figure 21 for the first stage Mach 0-7 vehicle are discussed in the following sub-sections. It is important to note that what is discussed herein does not make a complete hypersonic program. For example, it does not address the long-lead technical challenges for higher Mach air-breathing vehicle operation. It does not call out basic research needed for continual system level performance/operability improvements and maintaining a critical skill mix for future vehicle development challenges. Nor does it include University participation required to train, invigorate and maintain the workforce. Higher flight Mach number air-breathing vehicle, long-lead challenges include high-speed scramjet performance, structures and durability; high Mach turbine; advanced integral composite airframe/cryogenic fuel tank; and durable light-weight, high-temperature thermal protection materials and systems. Basic research focus should include efficient/effective fuel injector design, numerical and analytical modeling, multidisciplinary optimization, and wind tunnel test techniques. Better understanding of hypersonic unique physics will benefit, not enable future vehicle designs.

WBS Elements

1.0 Vehicle System
- 1.01 Customer Requirements Definition
- 1.02 Vehicle System Requirements Definition
- 1.03 Vehicle Systems Analysis
- 1.04 Vehicle Operations

2.0 Propulsion Systems—Performance
- 2.01 Dual Mode Ramjet/Scramjet
- 2.02 Lowspeed Propulsion System
- NA 2.03 Scramjet with LOX Augmentation
- 2.04 External Burning
- 2.05 External Rocket System
- 2.06 Flowpath Interaction

3.0 Propulsion Systems—Structural Architecture
- 3.01 Actively Cooled Engine Structure—Combustor
- 3.02 Actively Cooled Engine Structure—Inlet and Nozzle
- 3.03 Actively Cooled Engine Structure—Leading Edges
- 3.04 Thermal Protection System
- 3.05 High Temperature Propellant Piping
- 3.06 Cryogenic Propellant Piping
- 3.07 Primary Structure
- 3.08 Seals (static/dynamic)

4.0 Airframe—Structural Architecture
- 4.01 Fuselage Shell/H2 Tanks
- 4.02 LOX Tanks
- 4.03 Horizontal Control Surfaces
- 4.04 Vertical Control Surfaces
- 4.05 Payload Bay
- 4.06 Landing Gear Bay
- 4.07 Body Flaps
- 4.08 Seals

5.0 Thermal Protection Systems
- 5.01 Actively Cooled Leading Edges
- 5.02 Actively Cooled Fuselage Panels—Windward
- 5.03 Passively Cooled Leading Edges
- 5.04 Passively Cooled Fuselage Panels—Leeward
- 5.05 Passively Cooled Fuselage Panels—Windward
- 5.06 Passively Cooled Control Surface Panels

6.0 Mechanical Subsystems
- 6.01 Fuel System
- 6.02 Oxidizer System
- 6.03 Valves, Pressurization, Purge and Dump (VPP&D)
- 6.04 Auxiliary Power Unit (APU)
- 6.05 Electrical Power Generation and Control System (EPG&C)
- 6.06 Reaction Control System (RCS)
- 6.07 Hydraulics and High Pressure Actuation
- 6.08 Landing Gear
- 6.09 Air Vehicle Thermal Control System (AVTCS)
- 6.10 Hydrogen Pump
- 6.11 Oxidizer Pump

7.0 Avionics & Electrical Power/Subsystems
- 7.01 Integrated Avionics System (including IVHM)
- 7.02 Integrated Main Engine Control/Safety Monitor
- 7.03 GNC&T / Mission Design
- 7.04 Avionics Thermal Management
- 7.05 Avionics Power Source Development
- 7.06 Power Management and Control Grid
- 7.07 Air Data Systems
- 7.08 Pneumatic Actuation Controller
- 7.09 RLV Sensors

TRL
- 3 – 4
- 5 – 6
- 7 – 9

Figure 21. TRL Status for Low Mach Air-breathing Systems (Mach 7 1st Stage).

1. Air-Breathing Propulsion:

The turbine-based combination cycle engine system is a two-flowpath engine, in an arrangement "over-under" or separately integrated into the airframe. The low-speed engine is assumed to be a slightly modified F135 or F110 or equivalent hydrocarbon-fueled turbojet engine, with uninstalled thrust-to-weight (T/W) of about 7.5. This engine must dash to Mach 2.5, with about 1-minute operation required above Mach 2.

The high-speed engine is a hydrogen-fueled/ cooled ramjet/scramjet. Extensive databases exist for flowpath designs for good engine performance and operability, particularly from Mach 4 to 7. Key technical challenges for the thermal-throated dual-mode scramjet are low Mach number (M<4) performance and operability (TRL 4-5); demonstration of durable fixed or variable geometry metallic structure and seals (TRL 5); development and demonstration of robust engine controls for large operating range; optimization of aero-propulsion integration, and development of a 2000 psi expander cycle hydrogen fuel pump. The limited vehicle flight envelope may allow fixed geometry within the ram/scram flowpath, but variable geometry approaches are at reasonable levels (TRL 4-5) if needed. The TRL for physically-throated ramjets is very high based on numerous fielded missiles; however, availability of technical experts is a concern due to limited recent applications. No matter the type of ram/scramjet engine selected for the vision vehicle, a hydrogen fuel-cooled flight-weight engine must be tested to verify engineering prediction of system durability. These experiments will provide a test bed for instrumentation to support future integrated vehicle health management (IVHM). This development testing should be possible at small scale in an existing wind tunnel. Based on lessons learned in these systems tests, methods of testing critical flight-weight components at large scale using existing facilities must be developed. By limiting the maximum Mach number, this approach may be possible with existing facilities, whereas it will not be possible for Mach 10-15 concepts. By limiting the Mach number to 7, existing ground test facilities may be used to bring durable scramjet engine component technology toward TRL 6. Life cycle can be demonstrated at modest scale in combustion-heated facilities (like the 8ft. HTT), which allow sufficient test time for the structure to reach near equilibrium Mach 7 temperature. Flight mission-length duration tests can be performed at micro scale. (Life cycle testing was started in FY05, building on the technology developed by the USAF HyTech Program. This is an excellent demonstration of long-standing NASA-USAF cooperation, with the USAF focusing on hydrocarbon scramjet technology, and NASA on Hydrogen scramjet technology.)

Two additional propulsion technical challenges must also be addressed. Integration of the turbojet and ram/scram into a TBCC engine system (WBS 2.06) is a significant technical challenge (TRL 3-4). Integrated propulsion-airframe design/performance evaluation and thermal management (WBS 1.03) are also at a low TRL. This integration can and should first be tested in existing wind tunnels—providing "relevant environment." Wind tunnel tests of turbojet engines are acceptable system demonstration for TRL 6. The Mach 7 flight of the X-43 demonstrated that wind tunnels are a relevant environment for scramjet demonstration to TRL 6. Therefore TBCC engine tests in wind tunnels meet the TRL 6 (relevant environment) requirement. However, continual variation of flight Mach number from sea-level-static to Mach 7 can only be performed in flight. Also, flight forces closer attention to details often overlooked in ground tests. Low cost methods of testing and/or demonstrating these technologies may be possible. The simplest may be to fly the integrated system on a rocket booster, like the Russian Central Institute of Aviation Motors scramjet flying laboratory.

Integrated TBCC powered hypersonic vehicle TRL level of 6 cannot truly be achieved without a near-full scale flight test vehicle. However, completion of the above technology development provides a strong case to move to a large-scale research or prototype vehicle. Without first completing the above technology development and ground tests, a large scale research or prototype vehicle program may be doable, but it will be high risk, reminiscent of the National Aerospace Plane (NASP) Program.

External burning and external rocket systems are used in some first stage architectures. External burning must be performed at large scale, possibly requiring flight tests. The external rocket is discussed below.

2. High Temperature Materials and Thermal Protection System (TPS):

Vehicles designed for Mach 7 assume aluminum or titanium primary structure. Gamma Ti-Al or Beta Ti-Al structure could be incorporated if and when manufacturing technologies become available under other programs.

Some TPS may be required on the vehicle and engine. Baseline TPS are state of the art from the space shuttle. High temperature metallic, carbon-carbon or C/Si-C may be useful for some acreage TPS, operating within existing materials/coating limits. In addition, leading edges may require cooling for durability. Detailed system analyses for vision vehicles must be used to help identify specific technologies required and shortfalls. Technology to meet identified shortfalls can be ground demonstrated to TRL 6 for this Mach 7 limited first stage launch vehicles.

3. Propellant Tanks:

Flight weight fuel tanks for hydrocarbon fuel are state of the art. Cryo tanks, for liquid oxygen and liquid hydrogen, are assumed to be Al or Al-Li, with TRL 5-6. Integral or non-integral conformal Graphite-Epoxy tanks, if available

(TRL 3-4), would reduce tank weight, but are not required for this class of vehicle. Flight weight reusable metallic cryogenic tanks are the primary airframe technology requiring development. Large-scale flight-weight metallic tank fabrication and ground testing will elevate this technology to TRL 6.

4. Integrated Vehicle Design and MDO Tools:

A major challenge for hypersonic vehicle design is robust credible optimized-design simulations incorporating uncertainties for the intended mission. These tools must allow efficient relevant trades for vehicles operating over a large range of flight conditions. This challenge is significantly reduced when the vehicle Mach operating range is reduced. Confidence and "Analysis TRL" factors are elevated by appropriate data to validate the design tools.

The X-43 provided a large database for validation of aerodynamic and aerothermal design tools, scramjet propulsion performance and propulsion-airframe interactions. The major short-fall is TBCC-airframe integration and mode transition performance and operability. A secondary short-fall is the limited quantity and quality of experimental databases to validate transonic propulsion-airframe integration performance and operability.

Finally, the vision Mach 7 first-stage launch-vehicle design TRL, or design fidelity, is low. Notional concepts are more of a winged-body/wave-rider configuration, vis-à-vis lifting bodies required for Mach 12-15 air breathing operation. Higher lift/drag configurations may mitigate challenges associated with high takeoff speeds—such as tire technology. More detailed analyses, with higher fidelity tools discussed above are needed to define and guide vehicle technology requirements.

5. Expander Cycle Linear Aero-spike Rocket:

Another area requiring some development is the expander cycle hydrogen-oxygen linear aerospike tail rocket (WBS 2.05). It may be required for the first stage pull-up maneuver to set up conditions for stage separation, and for reusable second stage vehicles to facilitate integration of two winged stages. Significant development was accomplished during the NASP program, pushing the TRL to 5-6. Ground durability testing of such an integrated tail rocket system will focus and complete development of this technology.

6. Flight Testing:

Flight-testing is a natural evolution of any new aeronautical technology. Flight drives integration of all technologies required to complete a system—and generally developed separately before going to flight. Flight identifies challenges not generally known beforehand (unknown-unknowns). Flight generates customer, political and public interest. When to introduce flight-testing into a technology development program is an issue for thoughtful discussion. If funding is not highly constrained, flight-testing can move technology at a system level forward at a faster rate than likely without flight testing. If funding is constrained, careful consideration must be given before committing to flight research. Whatever budget unfolds, flight must be a part of hypersonic air-breathing technology development. The challenges and successes associated with flight-testing will continue to attract bright students into the sciences and engineering.

Flight-testing will be required for a few of the technology needs discussed. These include mid-large scale integrated combination engine performance, operability and durability, and validation of aero-propulsion integration. A subset of this would be durability testing of the large-scale scramjet engine. Another useful test would address scramjet flight controls over typical flight operating conditions. This could build on the X-43 and USAF's HyTech flight control efforts, expanding the flight envelop with a focus on both engine operability and engine durability sensors.

V. Summary and Conclusions

The 2nd and 3rd flights of the X-43 were successfully completed on March 27, and November 16, 2004. This was the world's first scramjet powered aircraft, and is recognized as the worlds fastest "jet powered aircraft." All phases of these two flights were performed as planned. The booster delivered the stack to the stage separation point at slightly low Mach and dynamic pressure. The stage separation system performed smoothly, accomplishing the first known successful non-symmetric, high-dynamic pressure, high Mach number stage separation, which is required for future hypersonic airbreathing launch systems. Research vehicle flight controls held angle of attack commanded to within a few tenths of a degree. Both vehicle drag and lift were slightly higher than predicted, but within the design uncertainty. The F2 vehicle accelerated under its own power for 15 miles in 11 seconds. The F3 vehicle demonstrated powered cruise at Mach 9.68, at 110,000 ft. altitude, covering 20 miles in 10.5 seconds of powered flight. Scramjet thrust measured matched prediction to within better than 2%. A huge, excellent quality database was generated, which is only now starting to be evaluated. Analyses and validation of design methods are continuing—but the conclusion is already clear—Scramjet powered vehicles can meet the performance claims and challenges of the next generation of air vehicles!

Hyper-X technology advancements have moved the nation toward its vision of safe, affordable airplane-like spacecraft. On a path toward the ultimate application, single stage to orbit, the X-43 flight is a small step. However, on a path to an entry-level air-breathing TSTO launch vehicle, which could compete for a large percent of current and projected missions, it is a large step. X-43 flight data confirmed the relevance of scramjet and powered vehicle wind tunnel testing in ground test facilities, and the adequacy of systems analysis/engineering for scramjet-powered vehicles. Combining the X-43 successes with other NASA and DOD program accomplishments, NASA and its contractors are closing in on the technologies required for a Mach 7 1st stage launch system. Technology development needs were defined, and will require flight-testing. Cost and time requirement for completing technology for an entry level reusable horizontal takeoff and landing capability is much less than required to achieve the NASP dream of single-stage to orbit. This technology is well within NASA's budget realities.

VI. References

[1]H. Julian Allen: "Hypersonic Flight and the Re-entry Problem," The Twenty-First Wright Brothers Lecture. Journal of the Aerospace Sciences, Vol. 25, No. 4, April 1958.

[2]Bilardo, V.J.; Hunt, J.L.; Lovell, N.T.; Maggio, G.; Wilhite, A.W.; and McKinney, L.E.: The Benefits of Hypersonic Air-breathing Launch Systems for Access to Space. AIAA 2003-5265. July 2003, Huntsville, AL.

[3]McClinton, C.R.; Andrews, E.H; and Hunt, J.L.: Engine Development for Space Access: Past, Present and Future. 26th Air-breathing Propulsion Subcommittee (APS) Meeting, Destin, FL 8-12 April 2001.

[4]McClinton, C.R. and Rausch, V.L.: Hyper-X Program Status. 26th Air-breathing Propulsion Subcommittee (APS) Meeting, Destin, FL 8-12 April 2002.

[5]Storch, A.R.; Ferlemann, S.M; Bittner, R.D.: Hyper-X, Mach 7 Scramjet Preflight Predictions versus Flight Results. 28th JANNAF Air-breathing Propulsion Subcommittee Meeting. Charleston, SC. June 13-17, 2005.

[6]Auslender, A.H.: "Scramjet Analysis Techniques," 28th JANNAF Air-breathing Propulsion Subcommittee Meeting. Charleston, SC. June 13-17, 2005.

[7]Ferlemann, S.M.; Voland, R.T.; Cabell, K, Whitte, D.; and Ruf, E.: Hyper-X Mach 7 Scramjet Pretest Predictions and Ground to Flight Comparison. AIAA 2005-3322. Presented at 13th International Space Planes and Hypersonic Systems and Technology Conference, Capua, Italy. May 2005.

[8]Ferlemann, P.: Hyper-X Mach 10 Scramjet Preflight Predictions vs. Flight Data. AIAA 2005-3352. Presented at 13th International Space Planes and Hypersonic Systems and Technology Conference, Capua, Italy. May 2005.

[9]Redifer, M.E.; Lin, Y.; Kelly, J.; Hodge, M.; and Barklow, C.: The Hyper-X Flight System Validation Program. Hyper-X Program Office Report: HX-849. 2003. (also: Hyper-X Fluid/Environmental Systems: Ground and Flight Operation and Lessons Learned. 28th JANNAF Air-breathing Propulsion Subcommittee Meeting. Charleston, SC. June 13-17, 2005.)

[10]Harsh, P.T.; Keel, L.C.; Castrogiovanni, A.; and Sherrill, R.T.: X-43 Vehicle Design and Manufacture. 28th JANNAF Air-breathing Propulsion Subcommittee Meeting. Charleston, SC. June 13-17, 2005. (See also: Keel, L.C.: X-43 Research Vehicle Design and Manufacture. AIAA 2005-3334. Harsh, P.T.; Keel, L.C.; Castrogiovanni, A.; and Sherrill, R.T.: X-43 Vehicle Design and Manufacture. 13th International Space Planes and Hypersonic Systems and Technology Conference, Capua, Italy. May 2005.)

[11]Keel, L.C.: X-43 Design and Manufacture (Mach 7 and 10). 28th JANNAF Air-breathing Propulsion Subcommittee Meeting. Charleston, SC. June 13-17, 2005.

[12]Joyce, P.J.; Pomroy, J.B. and Grindle, L.: The Hyper-X Launch Vehicle: Challenges and Design Considerations for Hypersonic Flight Testing. AIAA 2005-3333, Presented at 13th International Space Planes and Hypersonic Systems and Technology Conference, Capua, Italy. May 2005.

[13]Joyce, P.J.; and Pomroy, J.B.: Launch Vehicle Design Challenges for Hypersonic Flight Testing (Mach 7 and 10). 28th JANNAF Air-breathing Propulsion Subcommittee Meeting. Charleston, SC. June 13-17, 2005.

[14]X-43 Mishap Investigation Board: Report of Findings: X-43 Mishap. NASA Washington, DC. May 8, 2003.

[15]McClinton, C.R.; Rausch, V.L.; Nguyen, L.T.; and Sitz, J.R: "Preliminary X-43 Flight Test Results," IAC 04-V6-X42A 2, Nov. 2004.

[16]Jones, T.P.; Rock, K.E.; Cabell, K.; Nugent, M.; and Miranda, L.: Flight Test Performance Summary of the Propulsion System Controller of the X-43 Vehicles. 28th Air-breathing Propulsion Subcommittee Meeting. Charleston, South Carolina. June 2005.

[17]McAllister, D.W.; Neal, B.A.; Dowdell, D.B.; McMullen, W. and Fullerton, G.: Hyper-X Flight 2 and 3 Ground and Flight Operations. 28th JANNAF Air-breathing Propulsion Subcommittee Meeting. Charleston, SC. June 13-17, 2005.

[18]Corpening, G.; Marshall, L.; Sherrill, R.; and Nguyen, L.: A Chief Engineer's View of NASA's X-43 Scramjet Flight Test. AIAA 2005-3332. 13th International Space Planes and Hypersonic Systems Technology Conference, Capua, Italy. May 2005.

[19]Marshall, L.; Bahm, C.; Corpening, G.; and Sherrill, R.: X-43 Flight 3 Preparation and Results. AIAA 2005-3336. Presented at 13th International Space Planes and Hypersonic Systems and Technology Conference, Capua, Italy. May 2005.

[20]Baumann, E.A.: X-43 Guidance, Navigation and Control Challenges (Mach 7 and 10). 28th JANNAF Air-breathing Propulsion Subcommittee Meeting. Charleston, SC. June 13-17, 2005. (Also: Bahm, C.; Stovers, B.; Baumann, E.; Beck, R.; Bose, D.: X-43 Guidance, Navigation and Control Challenges. AIAA-2005-3275. 13th International Space Planes and Hypersonic Systems and Technology Conference, Capua, Italy. May 2005.)

[21]Morelli, E.A., Derry, S.D., and Smith, M.S. "Aerodynamic Parameter Estimation of the X-43A (Hyper-X) from Flight Test Data," AIAA-2005-5921, AIAA Atmospheric Flight Mechanics Conference, San Francisco, CA, August 2005.

[22]Karlgaard, C.D.; Tartabini, P.V. and Toniolo, M.D.: Hyper-X Post–Flight Trajectory Reconstruction. AIAA Atmospheric Flight Mechanics Conference. AIAA 2004-4829, Aug. 2004. (also: Karlgaard, C.; and Tartabini, P.V.: Best Estimated Trajectory Reconstruction for the X-43 Mach 7 and 10 Flights. 28th JANNAF Air-breathing Propulsion Subcommittee Meeting. Charleston, SC. June 13-17, 2005.)

[23]Del Corso, J.A; and the Hyper-X Staff: X-43 Flight 2 Data Release. HX-1076, NASA Langley Research Center, Hyper-X Program Office, March 2005.

[24]Del Corso, J.A; and the Hyper-X Staff: X-43 Flight 3 Data Release. HX-1077, NASA Langley Research Center, Hyper-X Program Office, May 2005.

[25]Vause, R.F.; Moore, D.F.; and Risner, N.: Weight Reduction Studies for the Hyper-X Mach 10 Vehicle. 28th JANNAF Air-breathing Propulsion Subcommittee Meeting. Charleston, SC. June 13-17, 2005.

[26]Martin, J.G.; Reubush, R.E; and Bose, D.M.: Hyper-X Stage Separation. 28th JANNAF Air-breathing Propulsion Subcommittee Meeting. Charleston, SC. June 13-17, 2005.

[27]Tartabini, P.V.; Martin, J.G.; Bose, D.M.; Thornblom, M; and Lien, J.P.: Mach 10 Stage Separation Analysis for the X-43-A. 28th JANNAF Air-breathing Propulsion Subcommittee Meeting. Charleston, SC. June 13-17, 2005.

[28]Blocker, W.: and Reubush, D.E.: X-43 Stage Separation System–A Flight Data Evaluation. AIAA 2005-3335. Presented at 13th International Space Planes and Hypersonic Systems Technology Conference, Capua, Italy. May 2005.

[29]Engelund, W.C.: Hyper-X/X-43 Aerodynamics: Results from the Mach 7 and Mach 10 Scramjet Flight Test. 28th JANNAF Air-breathing Propulsion Subcommittee Meeting. Charleston, SC. June 13-17, 2005.

[30]Engelund, W.C.: Hyper-X/X-43 Aerodynamics: Results from the Mach 7 and Mach 10 Scramjet Flight Tests. AIAA 2005-3405. Presented at 13th International Space Planes and Hypersonic Systems Technology Conference, Capua, Italy. May 2005.

[31]Special Section: Hyper-X. Journal of Spacecraft and Rockets. Vol. 38, Mo. 6, Pg. 801-853. Nov-Dec. 2001.

[32]Ferlemann, P.G.: Comparison of Hyper-X Mach 10 Scramjet Predictions and Flight. 28th JANNAF Air-breathing Propulsion Subcommittee Meeting. Charleston, SC. June 13-17, 2005.

[33]Ruf, E.G.; Cabell, D.W.; Witte, D.W.; and Shih, A.T.: Hyper-X Mach 7 Scramjet Ground to Flight Comparisons. 28th JANNAF Air-breathing Propulsion Subcommittee Meeting. Charleston, SC. June 13-17, 2005.

[34]Rogers, R.C.; Shih, A.T.; and Hass, N.E.: Hyper-X Mach 10 Engine Flowpath Testing: Ground to Flight Comparisons. 28th JANNAF Air-breathing Propulsion Subcommittee Meeting. Charleston, SC. June 13-17, 2005.

[35]Berry, S.A.; Daryabeigi, K; Auslender, A.H. and Bittner, R.D: Boundary Layer Transition on the X-43A Flight 2. 28th JANNAF Air-breathing Propulsion Subcommittee Meeting. Charleston, SC. June 13-17, 2005.

[36]Amundsen, R.M; Leonard, C.P.; and Bruce, W.E. III: Hyper-X Hot Structures Comparison of Thermal Analysis and Flight Data. 15th Thermal and Fluids Analysis Workshop, Pasadena, CA. Aug. 30, 2004

[37]Leonard, C.P; Bruce, W.; and Amundsen, R.M: Hyper-X Hot Structures Design and Comparison with Flight Data. 28th JANNAF Air-breathing Propulsion Subcommittee Meeting. Charleston, SC. June 13-17, 2005.

[38]Cuda, V.; and Woelfel, R.: Comparison of Hyper-X Engine Thermal Analysis and Flight Data. 28th JANNAF Air-breathing Propulsion Subcommittee Meeting. Charleston, SC. June 13-17, 2005.

[39]Leonard, C.; Amundsen, R.; and Bruce, W.: Hyper-X Hot Structures Design and Comparison with Flight Data. AIAA 2005-3438. 13th International Space Planes and Hypersonic Systems Technology Conference, Capua, Italy. May 2005.

[40]Jentink, T.N. and Ferlemann, P.G.: Mach 10 Tip-to-Tail Preflight Prediction, 28th JANNAF Air-breathing Propulsion Subcommittee Meeting. Charleston, SC. June 13-17, 2005.

[41]Meyer, B.M.: Tip to Tail CFD Analysis of the Mach 7 X-43 Flight 2 Aerodynamics at Tare and Powered Conditions. 28th JANNAF Air-breathing Propulsion Subcommittee Meeting. Charleston, SC. June 13-17, 2005.

[42]Rock, K.E.; Voland, R.T.; and Witte, D.W.: Hyper-X Mach 7 and 10 Scramjet Operation. 28th JANNAF Air-breathing Propulsion Subcommittee Meeting. Charleston, SC. June 13-17, 2005.

[43]NASP Phase 2D Final Scientific and Technical Report A011 (DI-MISC-08711/T) F33657-91-L-2012, Dec. 13, 1994.

[44]Hunt, J.L.; Ricketts, R.H. and McClinton, C.R.: Reference Technology Sets and Readiness Levels for Hypersonic Air-breathing Vehicles. JANNAF CS, APS, PSHS and MSS Joint Meeting. Monterey, CA, Nov.13-17, 2000.

[45]Brown, R.L.: Assessing Technology Readiness Using a Value Stream Process. Presented at NET Workshop on Processes for Assessing Technology Maturation and Determining Requirements for Successful Infusion into Programs. Marshall Space Flight Center, Sep. 16-18, 2003.

[46]Committee on National Aerospace Initiative, Air Force Science and Technology Board, Division on Engineering and Physical Sciences: Evaluation of the National Aerospace Initiative. National Research Council of the National Academies. The National Academies Press, Washington, D.C., April 2004.

[47]Bowcutt, K.G; and Hatakeyama, S.J.: Challenges, Enabling Technologies and Technology Maturity for Responsive Space. AIAA 2nd Responsive Space Conference. AIAA 2004-6005.

[48]Charles R. McClinton, C.R.; Shaw, R.J.; Mehta, U.; Naftel, J.CIAC 2004: Hyper-X: Foundation for Future Research. IAC V8.08. Oct. 20049. Fuchs, Ron: Why & Whither Hypersonics Research in the USAF. USAF Scientific Advisory Board, 2000.

[50]Tandy, David: Architecture C Limited LifeCycle Analysis. SAIC Presentation to NGLT, February 12, 2004.

[51]Schuh, J. R.; Ranslem,G. R.; Shunick,J. R.: Tests of Regeneratively-Cooled Components for Hypersonic Ramjet Propulsion Systems. Vol. I. Concept Test Rig Results. AFAPL-TR-68-125-Vol-1/2. Final Report, March, 1969.

[52]Bouchez, M; Falempin, F.; Levine, V.; Avrashkov, V.; and Davidenko, D.: French-Russian Partnership on Hypersonic Wide Range Ramjet. AIAA-2001-1872, Kyoto, Japan. April 2001.